

Electrical transport in deformed nanostrips: electrical signature of reversible mechanical failure

SOUMENDU DATTA¹(*), DEBASISH CHAUDHURI¹(**), TANUSRI SAHA-DASGUPTA¹ (***)
and SURAJIT SENGUPTA¹(**)

¹ *S.N. Bose National Centre for Basic Sciences - Block JD, Sector III, Salt Lake, Kolkata 700 098, India*

PACS. 73.40.-c – Electronic transport in interface structures.
PACS. 73.22-f – Electronic structure of nanoscale materials.
PACS. 62.25.+g – Mechanical properties of nanoscale materials.

Abstract. – We calculate the electrical conductivity of a thin crystalline strip of atoms confined within a quasi one dimensional channel of fixed width. The conductivity shows anomalous behavior as the strip is deformed under tensile loading. Beyond a critical strain, the solid fails by the nucleation of alternating bands of solid and *smectic* like phases accompanied by a jump in the conductivity. Since the failure of the strip in this system is known to be reversible, the conductivity anomaly may have practical use as a sensitive strain transducer.

Introduction: Deformation of nano meter sized wires and bars have been studied, using theoretical analysis as well as experiments, extensively in recent times [1–3]. Such studies are useful both for understanding deformation mechanisms in general and for their relevance in the construction of nano devices [2]. Single crystal nano bars and strips have been shown to fail on tensile loading conditions by the familiar necking mechanism [3] where an elastic instability leads to a reduction of the cross section of bar. While necking in bulk samples [4] occurs along with extensive plastic deformation caused by the motion of dislocations, in nano strips and beams, dislocations cannot be nucleated because of much higher elastic energy costs [5]. This leads to novel layering transitions where the solid thins down layer by layer [3] and finally fractures after attaining the thickness of an atomic chain.

The situation is somewhat different if the nano sized solid is confined within a rigid channel [6] so that the necking transition is prevented. In this case, with imposition of an external strain parallel to the confining walls, the solid fails by a series of layer transitions where the number of crystalline layers decreases by one, accompanied by the nucleation of bands of a fluid with strong orientational order. The remarkable fact is that this transition is completely reversible, such that a decrease of the tensile strain, immediately causes these failure bands to disappear and the solid heals itself automatically. In this Letter, we look at the electrical conductivity

(*) E-mail:soumendu@bose.res.in

(**) E-mail:debc@bose.res.in

(***) E-mail:tanusri@bose.res.in

(**) E-mail:surajit@bose.res.in

of a nano solid undergoing such a transition. Our motivation is to explore the possibility of a strong electrical signal at the reversible transition. We hope that such a signal, if it exists, would be useful for designing nano electro-mechanical devices [2].

The model: Since our aim here is to explore general principles rather than evaluate the properties of any particular system in any great detail, we have chosen a simple model system in two dimensions. Our calculations may be directly relevant for a strip of atoms adsorbed on a flat substrate and confined within a narrow straight channel (see Fig. 1 (a)), large enough to accommodate only a few atomic layers. The system geometry is generated by assuming hard disk “atoms” where particles i and j , interact with the *effective* interatomic potential $V_{ij} = 0$ for $|\mathbf{r}_{ij}| > d$ and $V_{ij} = \infty$ for $|\mathbf{r}_{ij}| \leq d$, where d is the hard disk diameter and $\mathbf{r}_{ij} = \mathbf{r}_j - \mathbf{r}_i$ the relative position vector of the particles [7,8]. In three dimensions, the corresponding hard sphere system has been used [9] in the past to model electrical properties of simple liquid metals with some success. The pure hard disk free energy is entirely entropic in origin and the only thermodynamically relevant variable for a system of N atoms in an area A is the number density $\rho = N/A$ or the packing fraction $\eta = (\pi/4)\rho d^2$. Accurate computer simulations [8] of hard disks show that for $\eta > \eta_f = .719$ the system exists as a triangular lattice which melts below $\eta_m = .706$. We consider a narrow channel in two dimensions of width L_y defined by hard walls at $y = 0$ and L_y ($V_{\text{wall}}(y) = 0$ for $d/2 < y < L_y - d/2$ and $= \infty$ otherwise) and length L_x with $L_x \gg L_y$. Periodic boundary conditions are assumed in the x direction.

Once the system geometry is generated by means of Monte Carlo simulations of “hard disk” atoms, we use the generated structure as the underlying atomic arrangement for which electrical transmittance is computed. A similar treatment has been used also in Ref. [9] viz. using structural information from the hard sphere system as inputs to a calculation of electrical properties of liquid metals. For computation of electrical transmittance, a tight-binding form of the electronic Hamiltonian

$$H = \sum_i \sum_j t_{ij} |i\rangle \langle j|$$

is assumed, with hopping interactions t_{ij} between atoms i and j . Two different forms of the distribution (Fig. 2) have been considered, to study the influence of hopping strength distribution on the transmittance. The considered distributions have a simple power-law behavior of the form $\frac{B}{r^\alpha}$ where r is the distance between the atoms in the unit of the lattice constant of the unstressed triangular lattice. $\alpha = 5$ for set I and $\alpha = 7$ for set II. B is taken as 2.0, so that for $r = 1.0$, the nearest neighbor separation in the unstressed lattice, the hopping interaction is set as 2.0 in some energy unit. The distribution is also assumed to have a cut-off range, so that beyond the second nearest neighbor distance the hopping vanishes.

To compute the electrical transmittance of the system, we attach conducting, semi-infinite, one-dimensional leads along the horizontal direction of the sample. A set of leads are attached at regular intervals at both ends of the sample. The purpose of these leads is to bear the incoming, reflected and transmitted waves into and away from the sample. The leads are described by one-dimensional, tight-binding, nearest-neighbor Hamiltonian of the form

$$H_{\text{lead}} = V_L \sum_i (|i\rangle \langle i+1| + |i+1\rangle \langle i|)$$

Deformation behavior: The effect of strain on the hard disk triangular solid at fixed L_y large enough to accommodate a small number of layers $n_l \sim 9-25$ has been studied in Ref. [6]. The stress [10], $\sigma = \sigma_{xx} - \sigma_{yy}$ in units of $k_B T/d^2$, versus strain, $\epsilon = (\eta_0 - \eta)/\eta$, curve is shown

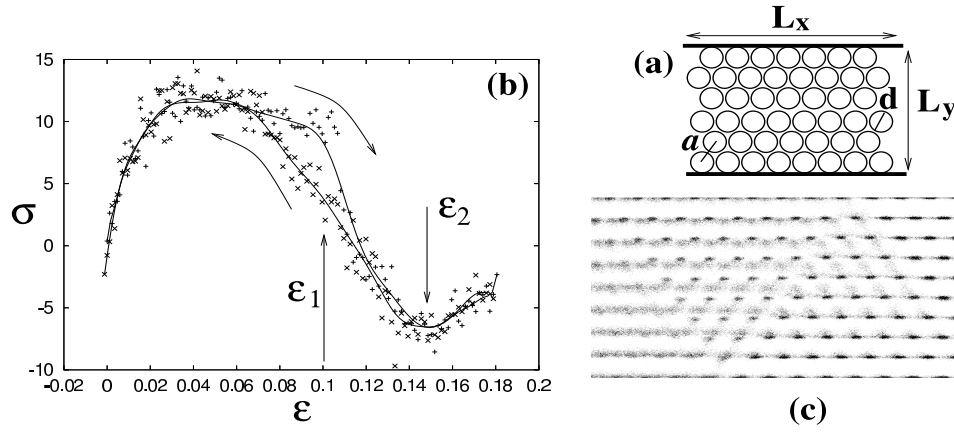


Fig. 1 – (a) The system geometry defining the quantities L_x , L_y , hard disk diameter d and the lattice parameter a . (b) The stress (σ) - strain (ϵ) curve as obtained from Monte Carlo simulations using $N = 60 \times 10$ hard disks [6]. The two sets of symbols + and \times correspond to the stress measured while the strain is increased and decreased respectively. The strain values ϵ_i , $i = 1, 2$ are marked. (c) Superposition of particle positions showing a crystal (right) - smectic interface. The number of layers in the crystalline region is larger by one. A smectic band is flanked by two such interfaces [6].

in Fig. 1(b). The packing fraction of the solid was taken to be $\eta_0 = 0.85$, a value deep in the solid phase. For $\eta = \eta_0$ ($\epsilon = 0$) the stress is purely hydrostatic with $\sigma_{xx} = \sigma_{yy}$ as expected. As the length, L_x , of the channel is increased keeping the width L_y fixed; initially, the stress increases linearly (Fig. 1(b)), flattening out at the onset of plastic behavior at $\epsilon \lesssim \epsilon_1$. At ϵ_1 , with the nucleation of smectic bands, σ decreases and eventually becomes negative. At ϵ_2 the smectic phase spans the entire system and σ is minimum. On further increase in strain, σ approaches zero from below (Fig. 1(b)) thus forming a Van der Waals loop. If the strain is reversed by increasing η back to η_0 the entire stress-strain curve is traced back with no remnant stress at $\eta = \eta_0$ showing that the plastic region is reversible. For $\epsilon_1 < \epsilon < \epsilon_2$ we observe that the smectic order appears within narrow bands (Fig. 1(c)). Inside these bands the number of layers is less by one and the system in this range of ϵ is in a mixed phase. The total size of such bands grows as ϵ is increased.

For every value of ϵ we store a number of hard disk configurations (~ 1000) which represent the instantaneous atomic positions. We use these configurations as structural information which are inputs to the electrical transport calculations to be described below. All transport quantities are averaged over these configurations so that our method closely corresponds to that followed in Ref. [9]. We proceed to obtain, in this fashion, the signature of smectic band formation on the conductivity of the strip.

Electrical transport: We compute the transmittance of the above described system by means of the vector recursion technique [11]. The essence of the vector recursion technique is the block tridiagonalization of the system Hamiltonian by changing to a new orthogonal set of vector basis, with the restriction that the lead Hamiltonian remains unchanged. In this last aspect, it differs from the standard Lancos method [12]. The numerical stability of this method [13] has been established in studying problems related to Anderson localization and quantum percolation model previously [14]. Below we describe the method briefly.

A representation of the original basis is column vectors, $\{|m\rangle\}$ of length $2\mathcal{N}$, where $\mathcal{N} = N/2$. Let us consider for the sake of demonstration, we have two leads, one incoming and

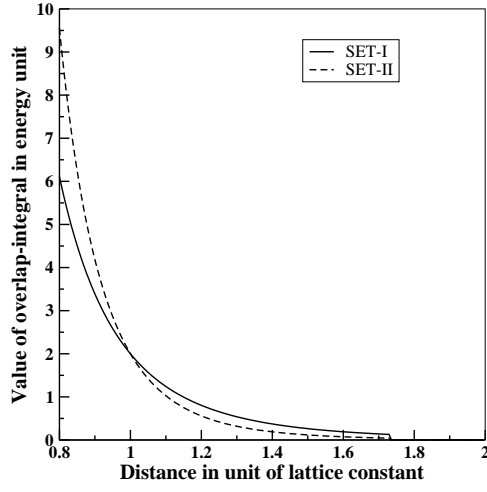


Fig. 2 – Two power-law distributions showing the variation of hopping-integral with distance

another outgoing connected to opposite ends of the sample at positions $|1\rangle$ and $|2\mathcal{N}\rangle$. A representation of the new vector basis is then matrices of size $2\mathcal{N} \times 2$. The members of the new basis are generated in the following way. The lead states are chosen to be,

$$|\Phi_n\rangle = \begin{pmatrix} |n\rangle \\ |2\mathcal{N} - n + 1\rangle \end{pmatrix}$$

with $n = 0, -1, -2, \dots, \infty$. The starting state within the system is chosen to be

$$|\Phi_1\rangle = \begin{pmatrix} |1\rangle \\ |2\mathcal{N}\rangle \end{pmatrix}$$

where $|1\rangle$ and $|2\mathcal{N}\rangle$ are the positions where the incoming and outgoing leads are attached. The subsequent members of the basis are generated from

$$\begin{aligned} B_2^\dagger |\Phi_2\rangle &= (H - A_1) |\Phi_1\rangle \\ B_{n+1}^\dagger |\Phi_{n+1}\rangle &= (H - A_n) |\Phi_n\rangle - B_n |\Phi_{n-1}\rangle \quad \text{for } n \geq 2 \end{aligned} \quad (1)$$

The matrix inner product is defined as

$$\{\Phi_\chi\}^{\mu\nu} = \sum_{i=1}^M \Phi_i^\mu \chi_i^\nu \quad \text{and} \quad \text{orthogonality as } \{\Phi|\chi\} = I$$

It can easily be shown that the 2×2 matrices A_n and B_n are block-tridiagonal members of the matrix representation of the Hamiltonian in the new basis:

$$A_n = \{\Phi_n | H | \Phi_n\} \quad B_n = \{\Phi_{n+1} | H | \Phi_n\}$$

so that the transformed Hamiltonian matrix can be divided in 2×2 blocks, with only non-zero diagonal and subdiagonal blocks.

The wavefunction $|\Psi\rangle$ may be represented in this new basis by a set $\{\psi_n\}$ so that $|\Psi\rangle = \sum_n \psi_n |\Phi_n\rangle$. These wavefunction amplitudes ψ_n also satisfy an equation identical with (1).

The solution of the Schrödinger equation in the leads are traveling Bloch waves of the form

$$\sum_m A \exp(\pm im\vartheta) |m\rangle$$

As the wave travels in the leads, the phase of its wavefunction changes by ϑ , where

$$\cos \vartheta = E/2V_L$$

E being the energy of the incoming electron [15]. In the incoming lead there will be an incoming wave of the form $\sum \exp(+im\vartheta) |m\rangle$ and a reflected wave of the form $\sum r(E) \exp(-im\vartheta) |m\rangle$. In the output lead there will be a transmitted wave $\sum t(E) \exp(-im\vartheta) |m\rangle$ [16], where $r(E)$ and $t(E)$ are the complex reflection and transmission coefficients. The boundary conditions may then be imposed from the known solution in the leads:

$$\begin{aligned} \psi_0 &= \begin{pmatrix} 1 + r(E) \\ t(E) \end{pmatrix} \\ \psi_1 &= \begin{pmatrix} \exp(i\vartheta) + r(E) \exp(-i\vartheta) \\ t(E) \exp(-i\vartheta) \end{pmatrix} \end{aligned}$$

The amplitude at the n th basis ψ_n may be written as

$$\psi_n = X_n \psi_0 + Y_n \psi_1,$$

where X_n and Y_n satisfy the same recurrence relation as (1) with EI replacing H and also satisfy the boundary conditions $X_0 = I$ and $X_1 = 0$, while $Y_0 = 0$ and $Y_1 = I$. Note that X and Y are 2×2 matrices.

This new basis terminates after $\nu = \mathcal{N}$ steps, as the rank of the space spanned by the original tight-binding basis remains unchanged after the transformation. Hence the recursion also terminates after ν steps. This gives an additional boundary condition

$$X_{\nu+1} \psi_0 + Y_{\nu+1} \psi_1 = 0_{2 \times 2}$$

If we now interchange the incoming and outgoing leads, we get a similar pair of equations for r' and t' , the transmission and reflection coefficients for wave incident from the second lead. Time reversal symmetry demands that t must be same for waves of the same energy incident from either lead so that $t = t'$. Solving these equations for the scattering S-matrix [17] for the sample region one have,

$$S = -(X_{\mathcal{N}+1} + Y_{\mathcal{N}+1} \exp(-i\vartheta))^{-1} (X_{\mathcal{N}+1} + Y_{\mathcal{N}+1} \exp(i\vartheta)) = \begin{pmatrix} r & t \\ t & r' \end{pmatrix}$$

Generalization of this methodology for the multi-lead case, as is the case for the present study, with M number of incoming leads and M number of outgoing leads is now a trivial task. The representation of new vector basis states formed out of repetitive application of recurrence relation are now matrices of sizes $2\mathcal{N} \times 2M$ with the first member chosen as

$$|\Phi_1\rangle = (|i_1\rangle |i_2\rangle \dots |i_M\rangle, |o_1\rangle |o_2\rangle \dots |o_M\rangle)$$

where $|i_k\rangle$ and $|o_k\rangle$ are the positions at which the incoming and outgoing leads attach to the system. The $2M \times 2M$ matrices A_n and B_n are the block tridiagonal representations of the

Hamiltonian in the new basis. The termination of the new basis occur after $\nu = 2\mathcal{N}/2M$ steps with the scattering S-matrix given by,

$$S = \begin{pmatrix} r_{11} & r_{12} & \cdots & r_{1M} & t'_{2M,1} & \cdots & t'_{2M,M} \\ \vdots & \vdots & \cdots & \vdots & \vdots & \cdots & \vdots \\ r_{M,1} & r_{M,2} & \cdots & r_{M,M} & t'_{M+1,1} & \cdots & t'_{M+1,M} \\ t_{M+1,1} & t_{M+1,2} & \cdots & t_{M+1,M} & r'_{M,1} & \cdots & r'_{M,M} \\ \vdots & \vdots & \cdots & \vdots & \vdots & \cdots & \vdots \\ t_{2M,1} & t_{2M,2} & \cdots & t_{2M,M} & r'_{11} & \cdots & r'_{1M} \end{pmatrix}$$

where we denote the reflection coefficient of the wavelet coming in from the i th incoming lead and reflected into the j th incoming lead by $r_{ij}(E)$, and the transmission coefficient of the same wavelet transmitted into the j' outgoing lead as $t_{ij'}(E)$.

The transmittance of the wavelet coming from the i th incoming channel is given by

$$T_i(E) = \sum_{j \in O} |t_{ij}(E)|^2 \quad \text{and the total transmittance } T = \sum_{i \in I} T_i$$

Here I and O denote the sets of incoming and outgoing leads, respectively.

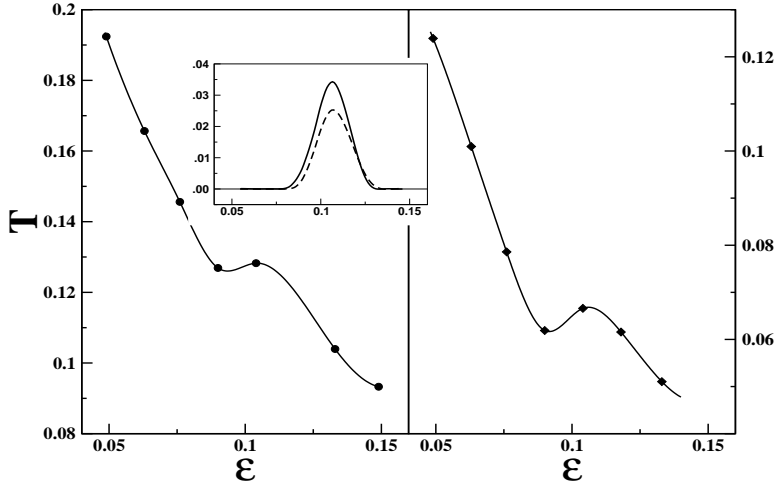


Fig. 3 – Variation of electrical transmittance (T) along the channel length with the variation of strain (ϵ) for two sets of hopping integrals (left panel: set I, right panel: set II). Inset shows the change in transmittance subtracting the $\sim 1/\epsilon$ behavior of the transmittance as a function of the increasing strain. The solid and dashed lines correspond to choice of hopping integrals, set II and set I respectively.

Discussion and conclusions: In Fig. 3, we show the transmittance of the system as a function of externally imposed strain. We notice the rather non-monotonic nature of the transmittance as the strain is increased. With imposed strain, the length of the system along the horizontal direction L_x increases, keeping the width L_y fixed. This results in larger separation between atoms lying along the horizontal direction and therefore smaller hopping interaction giving rise to net reduction in the transmitted current. The transmittance going roughly as $\sim 1/\epsilon$ (Fig. 3). This reduction continues until one reaches the strain value of

0.1 when the nucleation of smectic phase occurs. As explained above, within the smectic phase the number of atomic layers is reduced by one compared to that in the solid. The smectic phase with one less layer results in a decrease of the nearest neighbor distance *within* the layers and therefore to increased hopping interactions between atoms belonging to same layer and increased transmitted current along the horizontal direction as shown in the figure. On increasing the strain further, the width of the smectic band increases, thereby increasing the atomic separation along x - direction and decreasing the hopping interaction. Since this change is reversible, the transmittance retraces the curve as the strain is decreased. The change in transmittance is more obvious if one subtracts the overall $\sim 1/\epsilon$ behavior from the data. This may be achieved in real devices by measuring the differential conductance between two similarly strained strips one of which does not undergo the layering transition. Since the transition depends sensitively on the width of the strip [6] this can be easily arranged in practice.

For practical applications one needs the change in transmittance at the nucleation of the smectic phase to be as sharp as possible. Our study in this context indicates that sharpness of the transmittance jump depends crucially on the distribution of the hopping interaction strength. Changing the distribution from set-I to set-II, the value of the transmittance decreases in general due to the reduced hopping interaction in most of the cases, but at the same time also leads to more pronounced jump in the transmittance at the nucleation of the smectic phase. This indicates the necessity of engineering of proper materials to exploit this phenomenon in useful devices.

T. S. thanks DST for Swarnajayanti fellowship. S.S. acknowledges financial support from DST grant SP/S2/M-20/2001. S.D. and D.C. thank CSIR for financial supports.

REFERENCES

- [1] C. P. POOLE, F. J. OWENS, *Introduction to nanotechnology*, (Wiley, New Jersey) 2003
- [2] V. BALZANI, M. VENTURI, A. CREDI, *Molecular devices and machines: a journey into the nano world* (Wiley-VCH, Weinheim) 2003
- [3] NICOLÁS AGRAÏT, ALFREDO LEVY YEYATI, JAN M. VAN RUITENBEEK, *Physics Reports*, **377** (2003) 81
- [4] R. W. CAHN, P. HAASEN, *Physical Metallurgy, Third Edition* (Cambridge University Press, Cambridge) 1996
- [5] V. YAMAKOV, D. WOLF, S. R. PHILLIPOT, A. K. MUKHERJEE, H. GLEITER, *Nature Materials*, **1** (2002) 1
- [6] D. CHAUDHURI, S. SENGUPTA, *Phys. Rev. Lett.*, **93** (2004) 115702
- [7] B.J. ALDER, T.E. WAINWRIGHT, *Phys. Rev. B*, **127** (1962) 359
- [8] A. JASTER, *Physica A*, **277** (2000) 106
- [9] N. W. ASHCROFT, J. LEKNER, *Phys. Rev.*, **145** (1966) 83
- [10] O. FARAGO AND Y. KANTOR, *Phys. Rev. E*, **61** (2000) 2478
- [11] T.J.GORDIN AND R.HAYDOCK, *Phys.Rev. B*, **38** (1988) 5237.
- [12] R.HAYDOCK, *Solid State Physics, Volume 35*, edited by H. EHRENREICH, F. SIETZ AND D. TURNBULL (Academic Press, New York) 1980
- [13] T.J.GORDIN AND R.HAYDOCK, *Computer Physics Communications*, **64** (1991) 123.
- [14] I. DASGUPTA, T. SAHA AND A. MOOKERJEE, *Phys. Rev. B*, **47** (1993) 3097
- [15] Note that, in order to have propagating solutions, $|E| < 2V_L$. This sets the energy window. The Fermi energy of the lead-sample composite system is determined by the macroscopic lead Hamiltonian. For our calculation we have set $E=0$, which corresponds to half filled band in an one dimensional lead system with single s-band.

- [16] The process of vector recursion converts the lattice into an one-dimensional chain, which is then folded to clump two sites of the chain together to define the basis set $\{|\Phi_n\rangle\}$. For a chain with folded configuration (see Ref. [11] for details) both the reflected and transmitted waves move in opposite direction to that of the incident wave.
- [17] SUPRIO DATTA, *Electronic Transport in Mesoscopic System* (Cambridge University Press) 1995